


PAPER

[View Article Online](#)
[View Journal](#) | [View Issue](#)Cite this: *Dalton Trans.*, 2024, **53**, 15713Magnetocaloric effect in 1D-polymers bearing 15-metallacrown-5 {GdCu₅}³⁺ units and anionic oxalate complexes†Anna V. Pavlishchuk, ^{a,*} Sergey V. Kolotilov, ^a Matthias Zeller, ^b
Vitaly V. Pavlishchuk, ^a Fabrice Pointillart ^{*c} and Anthony W. Addison ^{*d}

Two complexes {[GdCu₅(GlyHA)₅(H₂O)₇Cr(C₂O₄)₃·11.02H₂O]_n (**1**) and {[GdCu₅(GlyHA)₅(H₂O)₆]μ₂-[Cu(C₂O₄)₂(H₂O)]₂μ₄-[Cu(C₂O₄)₂·15.8H₂O]_n (**2**)}, were obtained as outcomes of the reactions between the cationic hexanuclear {GdCu₅(GlyHA)₅}³⁺ 15-metallacrown-5 complex (where GlyHA²⁻ = glycinehydroxamate) and the anionic oxalate complexes K₃[Cr(C₂O₄)₃] or K₂[Cu(C₂O₄)₂]. Both **1** and **2** possess polymeric 1D-chain structures according to X-ray structural analysis. As a consequence of the geometric orientations of the donor atoms in the oxalates from [Cr(C₂O₄)₃]³⁻, the Cu₅ mean planes of neighboring 15-metallacrown-5 units {GdCu₅(GlyHA)₅}³⁺ are angled at 75.5° to each other, which leads to formation of a zig-zag motif in the 1D-chains of complex **1**. The centrosymmetric complex **2** contains two structurally different bis(oxalato)cuprate anions μ₂-[Cu(C₂O₄)₂(H₂O)]²⁻, for one of which, coordination to two adjacent {GdCu₅(GlyHA)₅}³⁺ units leads to formation of linear 1D-chains in **2**, while the second type, μ₄-[Cu(C₂O₄)₂]²⁻, is coordinated to four {GdCu₅(GlyHA)₅}³⁺ units, causing the cross-linking of single 1D-chains into a double-chain 1D coordination polymer. Studies of χ_MT vs. T data for **1** and **2** in a 2–300 K temperature range revealed the presence of both ferromagnetic and antiferromagnetic interactions amongst paramagnetic centres. The experimental χ_MT vs. T data for **1** were fitted using a model which takes into account exchange interactions between adjacent copper(II) ions, the Gd–Cu exchange interactions within {GdCu₅(GlyHA)₅}³⁺ units and additionally Gd–Cr exchange interactions. Fitting of the χ_MT vs. T data for **2** was not possible, since coordination of μ₄-[Cu(C₂O₄)₂]²⁻ to {GdCu₅(GlyHA)₅}³⁺ led to the non-equivalence of several Cu–Cu exchange interactions within the metallacrown units and hence a superfluity of fittable parameters. Complexes **1** and **2** are the first examples of 15-metallacrown-5 complexes demonstrating a magnetocaloric effect (–ΔS_M at 13 T reaches 24.26 J K^{–1} kg^{–1} at 5 K and 19.14 J K^{–1} kg^{–1} at 4 K for **1** and **2**, respectively).

Received 25th August 2024,
Accepted 2nd September 2024

DOI: 10.1039/d4dt02413c

rsc.li/dalton

^aL.V. Pisarzhevskii Institute of Physical Chemistry of the National Academy of Sciences of Ukraine, Prospect Nauki 31, Kyiv 03028, Ukraine.
E-mail: annpavlis@ukr.net, s.v.kolotilov@gmail.com,
shchuk@inphyschem-nas.com.ua

^bDepartment of Chemistry, Purdue University, 560 Oval Drive, West Lafayette, IN 47907-2084, USA. E-mail: zeller4@purdue.edu

^cUniv Rennes, CNRS, ISCR (Institut des Sciences Chimiques de Rennes) – UMR 6226, 35000 Rennes, France. E-mail: fabrice.pointillart@univ-rennes1.fr

^dDepartment of Chemistry, Drexel University, Philadelphia, PA 19104-2816, USA.
E-mail: addisona@drexel.edu

†Electronic supplementary information (ESI) available: Additional Fig. S1, showing a metallacrown fragment of the crystal structure of complex **2**, X-ray crystal structure refinement data (Table S1), and tables with structural information for **1** and **2** (Tables S2–S7). CCDC 2367413 (**2**–100 K), 2367414 (**1**) and 2379203 (**2**–RT). For ESI and crystallographic data in CIF or other electronic format see DOI: <https://doi.org/10.1039/d4dt02413c>

Introduction

Polynuclear clusters constructed from paramagnetic ions can exhibit a change of their isothermal magnetic entropy upon a change in applied magnetic field, known as the magnetocaloric effect (MCE).^{1,2} The interest in this phenomenon results from its potential application as paramagnetic molecular cryo-generators for the achievement of ultra-low temperatures, potentially providing an alternative to the use of scarce ³He.³ The magnetocaloric effect is usually characterised by an isothermal magnetic entropy change –ΔS_M or an adiabatic temperature change ΔT_{ad}.⁴ The magnetic entropy change is quite often derived indirectly from magnetisation studies.⁴ Significant magnetic entropy changes can be achieved in compounds possessing a high spin value for their ground state, since the maximum possible entropy change is defined as –ΔS_M = R ln(2S + 1), without any magnetic anisotropy.⁵

Complexes with high nuclearity obtained solely with 3d metal ions rarely demonstrate a significant magnetocaloric effect,⁴ usually because of antiferromagnetic exchange interactions between the paramagnetic ions and, in the case of many 3d metal ions, noticeable magnetic anisotropy.^{4,6}

Recent studies of Gd(III) clusters demonstrate that introduction of $S = 7/2$ Gd(III) ions with their seven unpaired electrons, negligible magnetic anisotropy and small exchange interactions due to the effective shielding of the 4f subshell has allowed the observation of record-high $-\Delta S_M$ values for molecular systems, comparable with that of commercially available garnet $\text{Gd}_3\text{Ga}_5\text{O}_{12}$.^{7,8}

Heteronuclear 3d–4f clusters containing Gd(III) ions often demonstrate a significant magnetocaloric effect, since weak ferromagnetic exchange interactions provide low-lying excited states potentially favorable for substantial magnetic cryogeneration.⁹ Introduction of Cu(II) ions into such polynuclear clusters is usually favorable for achieving significant $-\Delta S_M$ values, due to the weakly ferromagnetic Gd(III)–Cu(II) exchange interactions and negligible magnetic anisotropy of the Cu(II) ions.¹⁰ Polynuclear 15-metallacrown-5 complexes can serve as building blocks towards isolation of discrete polynuclear clusters or coordination polymers and in case of Gd(III)–Cu(II) metallamacrocycles, are known to demonstrate ferromagnetic exchange interactions.^{11–13} Despite such metallamacrocyclic systems being promising magnetic cryogenerants, magnetocaloric effects for 15-metallacrowns-5 have not yet been investigated. Previously, a heteronuclear GdFe_4 12-metallacrown-4 was investigated as a potential magnetic coolant. The achieved $-\Delta S_M = 7.3 \text{ J K}^{-1} \text{ kg}^{-1}$ at 3 K was however comparably small due to antiferromagnetic exchange interactions leading to a ground state with $S = 7/2$, a low density of low-lying excited spin states and the comparatively high molecular weight of this complex.¹⁴

Since the magnetic entropy change is usually given in gravimetric units, it is important to combine a high magnetic density with a small molecular weight, which can be best achieved by using small polydentate ligands.¹⁵ In this respect, since 15-metallacrown-5 complexes are usually obtained using α -substituted hydroxamic acids, glycinehydroxamic acid is a promising candidate for observing high gravimetric $-\Delta S_M$ values.

Numerous studies show that utilisation of diamagnetic linkers is unfavorable for significant MCE, however only diamagnetic linkers have so far been used for the design of polynuclear assemblies and coordination polymers with 15-metallacrown-5 building blocks.^{16–21} In this work we use 15-metallacrown-5 $\{\text{GdCu}_5(\text{GlyHA})_5\}^{3+}$ building blocks and for the first time combine them with paramagnetic linkers – anionic oxalate complexes $[\text{Cr}(\text{C}_2\text{O}_4)_3]^{3-}$ and $[\text{Cu}(\text{C}_2\text{O}_4)_2]^{2-}$, with the aim of creating products with higher magnetic density and investigating the magnetocaloric properties of these systems.

Results and discussion

Synthesis

The complexes $\{[\text{GdCu}_5(\text{GlyHA})_5(\text{H}_2\text{O})_7\text{-Cr}(\text{C}_2\text{O}_4)_3]\cdot 11.02\text{H}_2\text{O}\}_n$ (**1**) and $\{[\text{GdCu}_5(\text{GlyHA})_5(\text{H}_2\text{O})_6]\mu_2\text{-}[\text{Cu}(\text{C}_2\text{O}_4)_2(\text{H}_2\text{O})]\}_n$ (**2**) were obtained as the result of the reactions between previously reported heteropolynuclear Ln(III)–Cu(II) 15-metallacrown-5 $[\text{GdCu}_5(\text{GlyHA})_5(\text{CO}_3)(\text{NO}_3)(\text{H}_2\text{O})_5]\cdot 3.5\text{H}_2\text{O}$ ²² and the anionic oxalate complexes $\text{K}_3[\text{Cr}(\text{C}_2\text{O}_4)_3]$ or $\text{K}_2[\text{Cu}(\text{C}_2\text{O}_4)_2]$, respectively, in DMF–water mixtures. The complexes **1** and **2** formed as the result of complete anion metathesis in the initial 15-metallacrown-5 complex, in contrast to some previously described discrete assemblies based on 15-metallacrown-5 units and polycarboxylates.^{11–13,16–21} The complexes **1** and **2** possess electroneutral polymeric chains in their crystal structures. However, while in case of complex **1**, a zig-zag 1D-chain structure is observed, the centrosymmetric complex **2** also entails orthogonally cross-linking (themselves linear) 1D-chains.

The formation of dimeric^{12,17,18–20} or tetrameric^{16,19} discrete assemblies and coordination polymers^{11,16,18,20} utilising 15-metallacrown-5 building blocks was previously observed with a variety of anionic linkers, such as polycarboxylates^{11,16–20} or disulfonates.¹² To the best of our knowledge, there is only a single example described in the literature using diamagnetic $[\text{Fe}(\text{CN})_5(\text{NO})]^{2-}$ complex anions as linkers for 15-metallacrown-5 units, which led to the formation of a series of 2D-coordination polymers.²³ However, multiple examples of formation of discrete supramolecular assemblies or coordination polymers were reported utilising 9-metallacrown-3 and pentacopper(II) 12-metallacrown-4 building blocks with coordination complex anions acting as linkers.^{13,24,25}

Anionic oxalate complexes are among the most typical inorganic linkers for the construction of polynuclear discrete assemblies and coordination polymers with different dimensionalities.²⁶ Due to the rigidity of such paramagnetic linkers, they have successfully been employed in the rational construction of complexes with porous lattices²⁷ and compounds demonstrating interesting magnetic properties, such as molecular magnetism²⁸ or the magnetocaloric effect.²⁹

In this study we demonstrate that these anionic oxalate complexes lead to the formation of two different types of 1D-coordination polymers with heteropolynuclear 15-metallacrown-5 building blocks, the observed complexes being the first examples of 15-metallacrowns-5 displaying a magnetocaloric effect.

The polymeric 1D-chain of complex **1** contains 15-metallacrown-5 $\{\text{GdCu}_5(\text{GlyHA})_5(\text{H}_2\text{O})_7\}^{3+}$ building blocks, connected by tris(oxalato)chromate(III) anions $[\text{Cr}(\text{C}_2\text{O}_4)_3]^{3-}$, which coordinatively bridge two neighbouring metallamacrocyclic units (Fig. 1).

X-ray structures

$\{[\text{GdCu}_5(\text{GlyHA})_5(\text{H}_2\text{O})_7\text{-Cr}(\text{C}_2\text{O}_4)_3]\cdot 11.02\text{H}_2\text{O}\}_n$ complex (1). Reaction of the 15-metallacrown-5 complex $[\text{GdCu}_5(\text{GlyHA})_5(\text{CO}_3)(\text{NO}_3)(\text{H}_2\text{O})_5]\cdot 3.5\text{H}_2\text{O}$ ²² with $\text{K}_3[\text{Cr}(\text{C}_2\text{O}_4)_3]$ in DMF–water solution resulted in the formation of the 1D zig-zag coordination polymer $\{[\text{GdCu}_5(\text{GlyHA})_5(\text{H}_2\text{O})_7\text{-Cr}(\text{C}_2\text{O}_4)_3]\cdot 11.02\text{H}_2\text{O}\}_n$ (**1**) (Fig. 1).

The polymeric 1D-chain of complex **1** contains 15-metallacrown-5 $\{\text{GdCu}_5(\text{GlyHA})_5(\text{H}_2\text{O})_7\}^{3+}$ building blocks, connected by tris(oxalato)chromate(III) anions $[\text{Cr}(\text{C}_2\text{O}_4)_3]^{3-}$, which coordinatively bridge two neighbouring metallamacrocyclic units (Fig. 1).

The structural features of the metallamacrocyclic unit $\{\text{GdCu}_5(\text{GlyHA})_5\}^{3+}$ in **1** are typical of 3d–4f 15-metallacrown-5 complexes and have been described in detail previously.^{11,12,16–22,30–32} The $\{\text{GdCu}_5(\text{GlyHA})_5\}^{3+}$ units are built



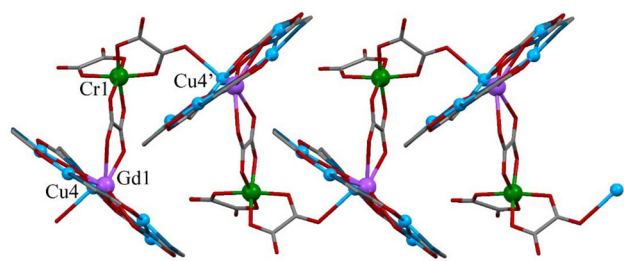


Fig. 1 Fragment of the crystal structure of complex **1**. In this and subsequent figures, water molecules and hydrogen atoms are omitted for clarity of presentation.

from five GlyHA²⁻ anions, which link five Cu(II) ions, forming metallamacrocyclic [Cu₅(GlyHA)₅] cores with Gd(III) ions located in the centre of the cyclic moiety (Fig. 1 and 2). The copper(II) ions in the {GdCu₅(GlyHA)₅}³⁺ units are located in a planar N₂O₂ coordination environment (nitrogen atoms are from hydroxamate and amino groups and oxygen atoms are from carbonyl and hydroxamate groups), while the Gd(III) ions are coplanarly coordinated by five hydroxamate oxygen atoms from within the Cu₅ unit.

According to calculations with the Shape 2.1³³ software, the ions Cu2 in **1** have distorted octahedral coordination environments, as a result of coordination of two water molecules in the apical positions of the Cu2 ions. The geometries of the copper(II) ions Cu1, Cu3 and Cu5 are completed to square pyramidal by coordination of water molecules in one of their apical positions. Similarly, ion Cu4 has a square pyramidal coordination geometry, with one of its apical positions occupied by oxygen atom O23 (Cu4–O23 = 2.587(5) Å), from a monodentate oxalate group from [Cr(C₂O₄)₃]³⁻ (Fig. 1 and 2, Tables S1–S3, ESI†).

A second oxalate group from the [Cr(C₂O₄)₃]³⁻ anion in **1** acts as a bidentate ligand to Gd(III) in an apical position through oxygen atoms O17 and O18 (Gd1–O17 = 2.691(3) Å)

and (Gd1–O18 = 2.535(3) Å)), though the third [Cr(C₂O₄)₃]³⁻ oxalate group remains non-coordinated to Cu(II) or Gd(III) ions. The Gd(III) ions in **1** are nine-coordinate, their coordination environments additionally involving oxygen atoms O11w and O13w (Gd1–O11w = 2.393(3) Å and (Gd1–O13w = 2.402(3) Å)) from two apically coordinated water molecules. The Gd1 ions in **1** have a coordination best described as CSAPR-9 – spherical capped square antiprismatic (*C*_{4v}) (Fig. S1, Table S4†).³³ All the bond lengths and angles in the metallamacrocyclic building block {GdCu₅(GlyHA)₅}³⁺ are typical of 15-metallacrown-5 complexes;^{11,12,16–22,30–32} selected structural parameters are given in Tables S1 and S2.†

The metallacrown units {GdCu₅(GlyHA)₅}³⁺ in **1** are slightly distorted from planarity, as is evident from the values of the average and largest deviations from the non-hydrogen atoms' Cu₅ mean planes, which are presented in Table S2.† The Cu₅ mean planes of adjacent metallacrown units are angled at 75.5 (1)° to one another, which leads to the formation of a zig-zag chain, in contrast to the previously reported linear polymeric assemblies with 15-metallacrown-5 units, where the mean planes of the adjacent metallamacrocyclic cores are oriented in a close to parallel manner.^{11,16,17}

Due to the peculiarities of the crystal lattice, there are voids between the 1D zigzag chains in **1**, which are filled by solvent water molecules. The total volume of solvent-accessible voids in **1** is 33.4% according to PLATON³⁴ calculations with a probe molecule of *r* = 1.4 Å (Fig. 3).

{[GdCu₅(GlyHA)₅(H₂O)₆]₂μ₂–[Cu(C₂O₄)₂(H₂O)]₂μ₄–[Cu(C₂O₄)₂·15.8H₂O]_n complex (**2**). The metathesis of [GdCu₅(GlyHA)₅(CO₃)(NO₃)(H₂O)₅·3.5H₂O]²² with K₂[Cu(C₂O₄)₂] in DMF–water solution resulted in formation of the double 1D-chain {[GdCu₅(GlyHA)₅(H₂O)₆]₂μ₂–[Cu(C₂O₄)₂(H₂O)]₂μ₄–[Cu(C₂O₄)₂·15.8H₂O]_n (**2**) (Fig. 4).

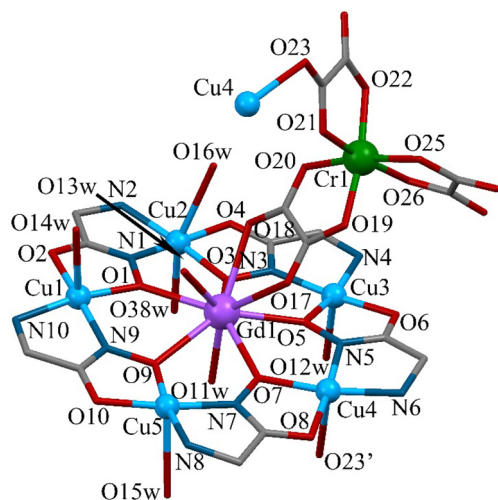


Fig. 2 Fragment of the crystal structure of complex **1** with the [GdCu₅(GlyHA)₅(H₂O)₇Cr(C₂O₄)₃] moiety.

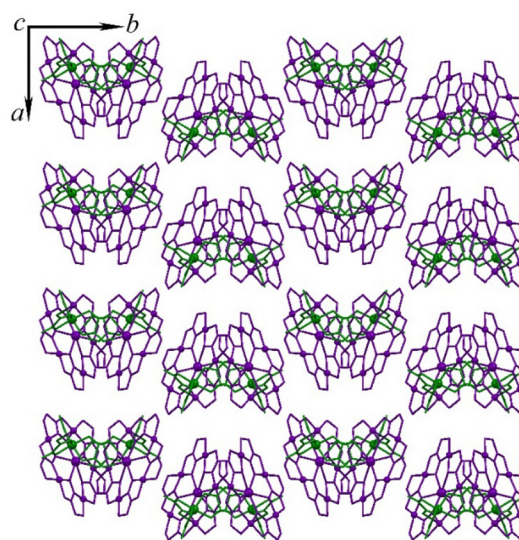


Fig. 3 Fragment of the crystal structure of **1**, viewed along the *c*-direction. The 15-metallacrown-5 cations {GdCu₅(GlyHA)₅}³⁺ are presented in purple and [Cr(C₂O₄)₃]³⁻ anions are shown in green.



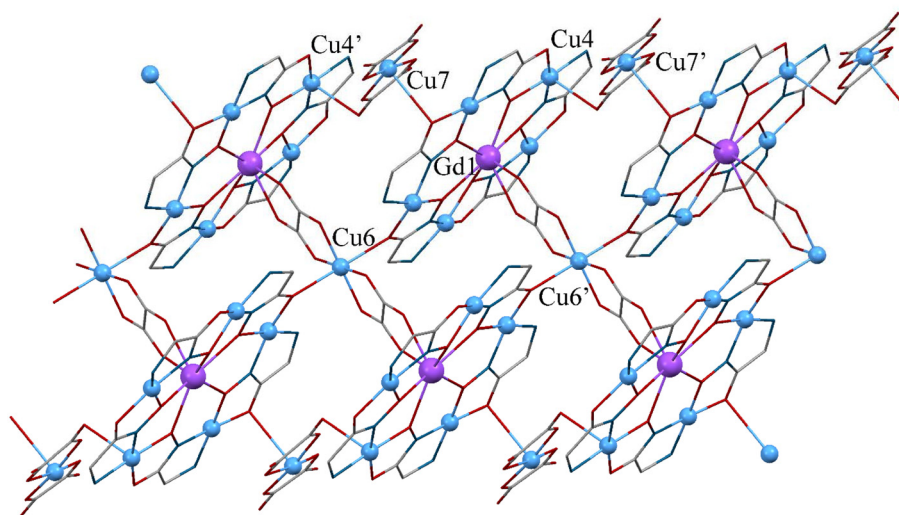


Fig. 4 Fragment of the crystal structure of complex 2 showing orthogonally cross-linked chains of $\{\text{GdCu}_5\}^{3+}$ units.

The polymeric 1D chain in complex 2 contains 15-metallacrown-5 $\{\text{GdCu}_5(\text{GlyHA})_5(\text{H}_2\text{O})_6\}^{3+}$ building blocks and two structurally different bis(oxalato)cuprate anions: the first type, $\mu_2\text{-}[\text{Cu}(\text{C}_2\text{O}_4)_2(\text{H}_2\text{O})]^{2-}$ is coordinated apically to two adjacent metallacrowns leading to the formation of linear 1D $\{\{\text{GdCu}_5(\text{GlyHA})_5(\text{H}_2\text{O})_6\}\mu_2\text{-}[\text{Cu}(\text{C}_2\text{O}_4)_2(\text{H}_2\text{O})]\}^+$ chains, while the second $\mu_4\text{-}[\text{Cu}(\text{C}_2\text{O}_4)_2]^{2-}$ structural type is bound to two adjacent $\{\{\text{GdCu}_5(\text{GlyHA})_5(\text{H}_2\text{O})_6\}\mu_2\text{-}[\text{Cu}(\text{C}_2\text{O}_4)_2(\text{H}_2\text{O})]\}^+$ 1D-chains by coordinating to four metallacrown building blocks (two from each 1D-chain). As a result, the two single 1D chains are linked pairwise into a double 1-D chain.

The structure of the metallacrown units $\{\text{GdCu}_5(\text{GlyHA})_5\}^{3+}$ in 2 is generally similar to the one in 1 in the equatorial coordination sphere (Fig. 5). All Cu(II) ions in the metallama-

crocyclic cores $\{\text{GdCu}_5(\text{GlyHA})_5\}^{3+}$ are distorted square-pyramidal pentacoordinate (Table S7†). Outside the equatorial coordination sphere, the apical positions of copper ions Cu1–Cu3 and Cu5 are occupied by coordinated water molecules, while the apical position of Cu4 is occupied by the oxalate oxygen atom O21 ($\text{Cu4-O21} = 2.512(3) \text{ \AA}$) from the apically coordinated $\mu_2\text{-}[\text{Cu}(\text{C}_2\text{O}_4)_2(\text{H}_2\text{O})]^{2-}$. The second oxalate group of the first type of bis(oxalato)cuprate anion in 2 remains uncoordinated. The μ_2 -bridging mode of $\mu_2\text{-}[\text{Cu}(\text{C}_2\text{O}_4)_2(\text{H}_2\text{O})]^{2-}$, which leads to the formation of 1D-chains, is observed due to the coordination of the Cu7 ions in the bis(oxalato)cuprate by the carbonyl oxygen atom O8' from an adjacent metallacrown cation ($\text{Cu7-O8}' = 2.731(2) \text{ \AA}$).

The Gd(III) ions in 2 are nine-coordinate and similarly to 1, their coordination environments correspond to a spherically-capped square antiprism (CSAPR-9 , C_{4v}) (Fig. S3, Table S4†). The second type of bis(oxalato)cuprate anion $\mu_4\text{-}[\text{Cu}(\text{C}_2\text{O}_4)_2]^{2-}$ links two adjacent 1D-chains $\{\{\text{GdCu}_5(\text{GlyHA})_5(\text{H}_2\text{O})_6\}\mu_2\text{-}[\text{Cu}(\text{C}_2\text{O}_4)_2(\text{H}_2\text{O})]\}^+$ due to the bidentate coordination of each oxalate anion to Gd1 ions through oxygen atoms O13 and O14 ($\text{Gd1-O13} = 2.517(5) \text{ \AA}$ and $\text{Gd1-O14} = 2.458(2) \text{ \AA}$). The coordination sphere of Gd1 is completed to nonacoordinate by two apically coordinated water molecules O15w and O29w ($\text{Gd1-O15w} = 2.375(2) \text{ \AA}$ and $\text{Gd1-O29w} = 2.737(4) \text{ \AA}$) (Table S6†).

The second structural type of bis(oxalato)cuprate $\mu_4\text{-}[\text{Cu}(\text{C}_2\text{O}_4)_2]^{2-}$ in complex 2 is centrosymmetric and displays coordination to four metallacrown units from two adjacent 1D-chains, causing formation of the double 1D-chains in 2. In addition to bidentate coordination of each oxalate anion in $\mu_4\text{-}[\text{Cu}(\text{C}_2\text{O}_4)_2]^{2-}$ to Gd1 ions, the Cu6 ions in this bis(oxalato)cuprate are coordinated to two carbonyl oxygen atoms O10' from two $\{\text{GdCu}_5(\text{GlyHA})_5\}^{3+}$ units ($\text{Cu6-O10}' = 2.341(2) \text{ \AA}$).

Thus, the first structural type of bis(oxalato)cuprate $\mu_2\text{-}[\text{Cu}(\text{C}_2\text{O}_4)_2(\text{H}_2\text{O})]^{2-}$ acts as a bridge between two adjacent metallacrown cations. The copper(II) ions Cu7 are hexacoordinate,

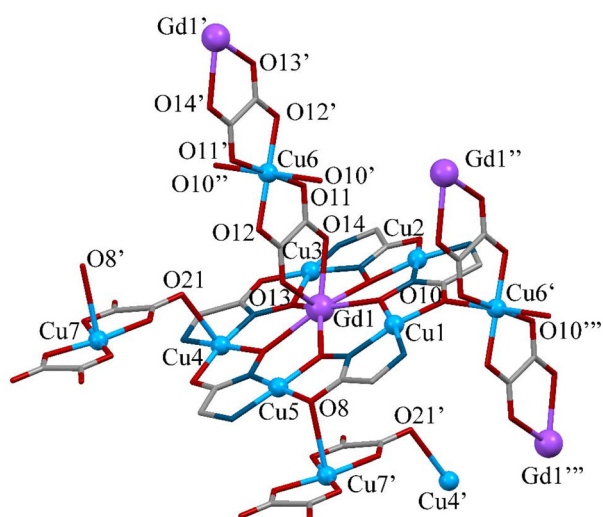


Fig. 5 Fragment of the crystal structure of complex 2 demonstrating the coordination of the $[\text{Cu}(\text{C}_2\text{O}_4)_2]^{2-}$ anions to the $\{\text{GdCu}_5(\text{GlyHA})_5\}^{3+}$ moiety.



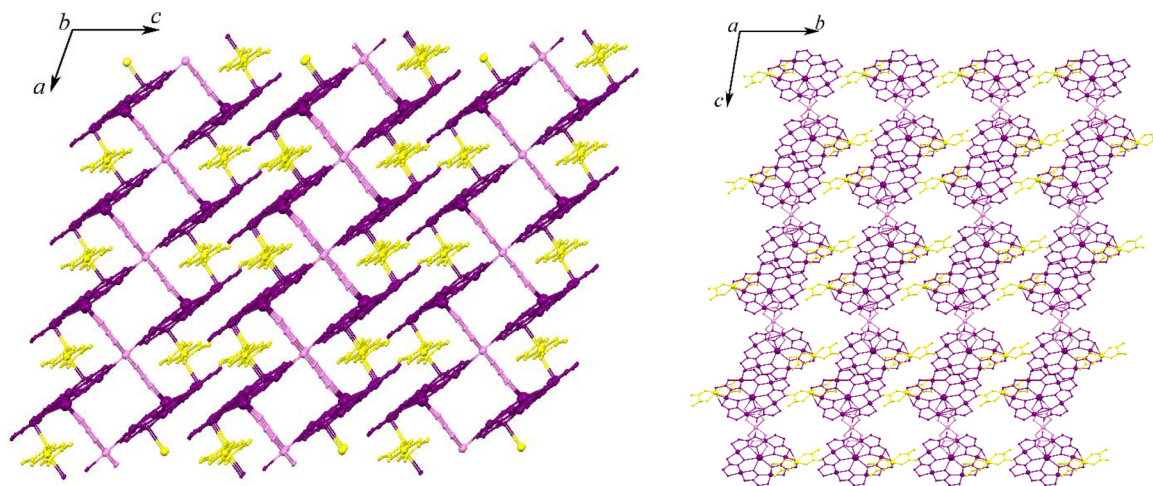


Fig. 6 Fragment of the crystal structure of **2**, viewed along the *b* (left) and *a* (right) directions. Hydrogen atoms and both coordinated and lattice water molecules are omitted for clarity of presentation. The 15-metallacrown-5 cations $\{\text{GdCu}_5(\text{GlyHA})_5\}^{3+}$ are in purple, while $\mu_4\text{-}[\text{Cu}(\text{C}_2\text{O}_4)_2]^{2-}$ and $\mu_2\text{-}[\text{Cu}(\text{C}_2\text{O}_4)_2]^{2-}$ are shown in pink and yellow, respectively.

with one apical position of Cu7 occupied by coordinated water molecule O26w and the other involved in formation of a 1D-chain due to the coordination of carbonyl oxygen atom O8' from $\{\text{GdCu}_5(\text{GlyHA})_5\}^{3+}$ units. The copper(II) ions in the second structural type of bis(oxalato)cuprate $\mu_4\text{-}[\text{Cu}(\text{C}_2\text{O}_4)_2]^{2-}$, are also hexacoordinate. Two apical positions of Cu7 ions contain two carbonyl oxygen atoms O10' from two metallacrown moieties. The centrosymmetric anion $\mu_4\text{-}[\text{Cu}(\text{C}_2\text{O}_4)_2]^{2-}$ binds four metallacrown cations leading to formation of the double 1D-chain.

The observed bond lengths and angles in the $\{\text{GdCu}_5(\text{GlyHA})_5\}^{3+}$ metallacrown unit are typical of 15-metallacrown-5 complexes;^{11,12,16–22,30–32} selected structural parameters are listed in Tables S2 and S6 (ESI).†

Similarly to complex **1**, the metallacrown unit $\{\text{GdCu}_5(\text{GlyHA})_5\}^{3+}$ in **2** is also almost planar (Table S2). The total volume of solvent-accessible voids in complex **2** is 22.0% ($r = 1.4$ Å probe radius)³⁴ (Fig. 6).

Stability of the crystalline assemblies

Crystal structures were obtained at 100 K, from crystals freshly taken from mother liquor. The high degree of solvation indicated a possibility of desolvation of the crystalline assemblies, *i.e.* a loss of solvating water molecules upon removal of the crystals from the mother liquor that they had been grown in. To test for a possible change of structure upon warming to room temperature, powder XRD data were collected for thoroughly ground and air-dried samples for both compounds at room temperature.

For complex **1**, the room temperature powder pattern provided a close match for the 100 K structural data. A Rietveld refinement plot is given in Fig. S6,† and additional refinement details are given in the ESI.† Unit cell parameters changed slightly to *ca.* $a = 13.62$, $b = 25.44$, $c = 14.91(8)$ Å and $\beta = 106.2^\circ$. The volume of the unit cell expanded very slightly by less than

0.5%, from 4939 to 4962 Å³. The overall good fit, and the very similar cell volume indicate that the structure of the air-dried sample is very little changed from the 100 K single crystal structure.

For complex **2**, the observations were different. Powder patterns for a well-ground sample dried at room temperature had very little resemblance to a pattern simulated from the 100 K single crystal data, even after allowances for unit cell expansion or other slight structural changes. Crystals of complex **2** were thus investigated in more detail by single crystal XRD. A crystal from a fresh crystallization batch was taken from the crystallization mother liquor and the structure at 100 K was confirmed for this crystal. The crystal was then gradually warmed at a rate of 6° C per minute to room temperature (298 K). Re-determination of the unit cell parameters indicated a substantial change to unit cell axes and angles (Table S9†). The unit determination was repeated several times, until no change in unit cell parameters was observed anymore (*ca.* 1 h at 298 K), and then the crystal structure was redetermined at 298 K.

The structures were similar enough to allow a structure solution from the 100 K dataset by isomorphous replacement. The arrangement of the 15-metallacrown-5 units and bridging $\mu_4\text{-}[\text{Cu}(\text{C}_2\text{O}_4)_2]^{2-}$ anions were largely unchanged. However, *ca.* 9 of the 24 previously present water molecules were not observable anymore and could also not be accounted for as diffuse highly disordered solvent content (12 water molecules could be refined and a Platon Squeeze procedure accounted for 3 more water molecules in a 4% pore volume). The $\mu_2\text{-}[\text{Cu}(\text{C}_2\text{O}_4)_2]^{2-}$ anion was found to be highly dynamic, with one of the oxalates swinging by nearly the entire length of the ligands (>2 Å). Additional structural details for complex **2** collected at room temperature are given in the ESI (Table S10, Fig. S8–S10†). Thus, this crystal lost about one-third of its water content (*ca.* 37.5%) when warmed to room temperature, or *ca.*



5.4% of its original molecular weight. The volume of the unit cell shrank from 2139.3(5) to 1901.3(9) Å³, *ca.* 11% of the original volume.

The loss of the water molecules upon warming to room temperature makes the structural change from the 100 K to the partially desolvated structure irreversible. Attempts to cool partially desolvated crystals back to 150 or 100 K to obtain better quality structural data resulted in strain buildup and fragmentation of the crystal.

To verify the purity of the original material, powder XRD data for complex **2** were obtained for freshly prepared non-ground sample soaked in water. Data collected in this manner closely resemble those for the expected structure from the 100 K single crystal structure. A Rietveld refinement plot is given in Fig. S7, and additional refinement details are given in the ESI.†

Magnetic properties

The magnetic properties of complexes **1** and **2** were studied in a dc magnetic field in the temperature range 2–300 K. The room temperature value of $\chi_M T$ for complex **1** (12.07 cm³ mol^{−1} K) is somewhat higher than the expected spin-only value (11.63 cm³ mol^{−1} K for five non-interacting Cu(II) ions ($S_{\text{Cu}} = 1/2$), one Gd(III) ion ($S_{\text{Gd}} = 7/2$) and one Cr(III) ion ($S = 3/2$) with $g_{\text{Cu}} = g_{\text{Gd}} = g_{\text{Cr}} = 2.00$) (Fig. 7). A temperature decrease to 36 K leads the $\chi_M T$ value to fall to 10.74 cm³ mol^{−1} K, which indicates the presence of the usual antiferromagnetic exchange interactions in the metallamacrocyclic core. With further temperature decrease, the $\chi_M T$ value grows to a maximum value of 11.24 cm³ mol^{−1} K at 5 K, which can be attributed to ferromagnetic exchange interactions between paramagnetic centres. A further temperature decrease to 2.0 K leads to the $\chi_M T$ value for **1** dropping to 10.90 cm³ mol^{−1} K at 2.0 K (Fig. 7).

The magnetic properties of the 1D-coordination polymer **1** can be described using a {GdCu₅(GlyHA)₅(Cr(C₂O₄)₃)} fragment, in which the [Cr(C₂O₄)₃]^{3−} anion is bidentately linked to Gd(III) (Fig. 2 and S4†). The possible exchange interaction between Cr1 ion and Cu4' from adjacent 15-metallacrown-5 fragment in **1** was neglected, since coordination of [Cr(C₂O₄)₃]^{3−} anions in apical positions of Cu(II) ions usually results only in small exchange interactions between Cr(III) and Cu(II) ions.^{35–37}

The observed $\chi_M T$ vs. T data were fitted using a model based on the three- J spin Hamiltonian (1), which takes into account both Gd–Cu and Cu–Cu exchange interactions in the {GdCu₅}³⁺ metallacrown core and, in addition, exchange interactions between the Gd(III) and Cr(III) ions from the coordinated [Cr(C₂O₄)₃]^{3−} anion (Fig. S4†):

$$\begin{aligned} \hat{H}(\{\text{GdCu}_5\}\text{Cr}) = & -2J_{\text{Gd-Cu}}(\hat{S}_{\text{Gd}} \cdot \hat{S}_1 + \hat{S}_{\text{Gd}} \cdot \hat{S}_2 \\ & + \hat{S}_{\text{Gd}} \cdot \hat{S}_3 + \hat{S}_{\text{Gd}} \cdot \hat{S}_4 + \hat{S}_{\text{Gd}} \cdot \hat{S}_5) \\ & -2J_{\text{Cu-Cu}}(\hat{S}_1 \cdot \hat{S}_2 + \hat{S}_2 \cdot \hat{S}_3 + \hat{S}_3 \cdot \hat{S}_4 \\ & + \hat{S}_4 \cdot \hat{S}_5 + \hat{S}_5 \cdot \hat{S}_1) - 2J_{\text{Gd-Cr}}\hat{S}_{\text{Gd}} \cdot \hat{S}_{\text{Cr}} \end{aligned} \quad (1)$$

where $J_{\text{Gd-Cu}}$ is the exchange integral between Gd(III) and Cu(II) ions, $J_{\text{Cu-Cu}}$ between adjacent Cu(II) ions in the metallamacro-

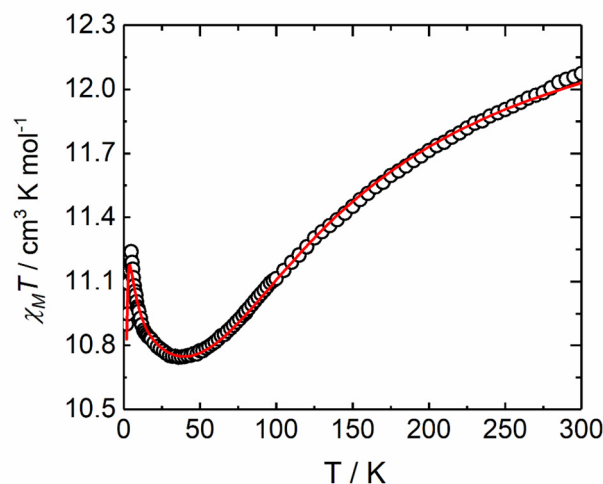


Fig. 7 Thermal dependence of the molar magnetic susceptibility for **1**, presented per {GdCu₅}Cr moiety (open black circles). The red line represents the best fit with parameters obtained with a theoretical model based on Hamiltonian (1) (see main text).

cycle, $J_{\text{Gd-Cr}}$ is the exchange integral between Gd(III) and Cr(III) ions; \hat{S}_i are spin operators for the Cu(II) ions, while \hat{S}_{Gd} and \hat{S}_{Cr} are spin operators for the Gd(III) and Cr(III) ions, respectively. The $\chi_M T$ vs. T data for **1** were fitted using the PHI software.³⁸ The best correspondence between experimental and fitted data was observed with the following parameter values (Fig. 9): $J_{\text{Cu-Cu}} = -59.6(3)$ cm^{−1}, $J_{\text{Gd-Cu}} = +0.380(7)$ cm^{−1}, $J_{\text{Gd-Cr}} = +0.074(2)$ cm^{−1}, $g_{\text{Gd}} = 2.050(1)$, $g_{\text{Cu}} = 2.344(5)$, $g_{\text{Cr}} = 1.98$ (fixed) and $zJ' = -0.0120(1)$ cm^{−1}, with $R^2 = 3.12 \times 10^{-5}$.³⁹

Complex **1** is the third example of a 15-metallacrown-5 utilizing the {GdCu₅}³⁺ fragment with values reported for exchange interactions between paramagnetic centers. The values of Cu(II)–Cu(II) exchange interactions obtained for **1** are comparable to previously reported ones of $-54(4)$ and $-61.0(5)$ cm^{−1} for Gd(III)–Cu(II) 15-metallacrowns-5,^{11,12} and are typical for {LnCu₅}³⁺ fragments with different Ln(III) ions, with $J_{\text{Cu-Cu}}$ ranging from $-44.1(2)$ to $-68(4)$ cm^{−1}.^{16,17,40,41} The $J_{\text{Gd-Cu}}$ values in **1** are also comparable to previously observed values ($+0.60(2)$ and $+0.85(1)$ cm^{−1}) for 15-metallacrowns-5 bearing a {GdCu₅}³⁺ unit.^{11,12} Weak ferromagnetic Gd(III)–Cu(II) exchange interactions, which usually vary from a tenth of a wavenumber to a few wavenumbers, have been reported for various classes of coordination compounds with different nuclearities of complexes and different bridging groups between Gd(III) and Cu(II) ions.^{42–45}

To the best of our knowledge, there are no reported ferromagnetic exchange interactions between Gd(III) and Cr(III) ions which exceed 0.3 cm^{−1},⁴⁶ whereas examples of weak antiferromagnetic exchange interactions for Gd(III) and Cr(III) ions, especially in cases of single atom bridges, are more common in comparison with Gd(III)–Cu(II) exchange interactions.^{46a,47}

The $\chi_M T$ value at 300 K for complex **2** (20.00 cm³ mol^{−1} K) is slightly lower compared to a theoretically calculated spin-only value (20.63 cm³ mol^{−1} K for thirteen non-interacting Cu(II)



ions ($S_{\text{Cu}} = 1/2$) and two Gd(III) ions ($S_{\text{Gd}} = 7/2$) with $g_{\text{Cu}} = g_{\text{Gd}} = 2.00$ (Fig. 8). With decreasing temperature, the value of $\chi_{\text{M}}T$ gradually falls, reaching a minimum of $17.86 \text{ cm}^3 \text{ mol}^{-1} \text{ K}$ at 40 K, evidencing the existence of antiferromagnetic exchanges between paramagnetic centres in complex 2. Further temperature decrease leads to the growth of the $\chi_{\text{M}}T$ value, with it reaching a maximum of $20.12 \text{ cm}^3 \text{ mol}^{-1} \text{ K}$ at 2 K, which, again, can be attributed to ferromagnetic exchange interactions between Gd(III) and Cu(II) ions in the metallamacrocyclic cores (Fig. 8).

The observed $\chi_{\text{M}}T$ vs. T data for complex 2 cannot be fitted using the $2J$ -model,^{11,12} which includes equivalent exchange interactions between adjacent Cu(II) ions in the metallamacrocyclic core. The equatorial coordination of $\mu_4\text{-}[\text{Cu}(\text{C}_2\text{O}_4)_2]^{2-}$ leads to close contacts between the Cu6 ion from $\mu_4\text{-}[\text{Cu}$

$(\text{C}_2\text{O}_4)_2]^{2-}$ and two copper(II) ions Cu1 in two 15-metallacrown-5 cores connected by a bridging bis(oxalato)cuprate. The Cu6 and Cu1 ions are separated only by the bridging carbonyl oxygen atom O8, which leads to a Cu6–Cu1 = $3.7695(5) \text{ \AA}$ contact, which is shorter than for the adjacent Cu–Cu in the metallamacrocyclic core, which range from $4.5594(7)$ to $4.6170(7) \text{ \AA}$. The ions Cu6 and Cu2 are connected through a triatomic –O–C–N– bridge, which leads to a longer Cu6–Cu2 contact ($6.0464(6) \text{ \AA}$). The existence of short Cu6–Cu1 contacts creates the necessity of taking into account the $J_{3\text{Cu-Cu}}$ exchange interactions between copper ion Cu6 from $\mu_4\text{-}[\text{Cu}(\text{C}_2\text{O}_4)_2]^{2-}$ and Cu1 from the metallamacrocyclic core; this makes exchange interactions between adjacent Cu–Cu core ions non-equivalent, leading to at least two different $J_{\text{Cu-Cu}}$ exchange interactions inside the 15-metallacrown-5, due to the symmetry lowering of the metallamacrocycle (Fig. 9). The large attendant matrices defeated our attempts to fit the data for complex 2 with the PHI software.

Magnetocaloric effect

The evaluation of a possible magnetocaloric effect in complexes 1 and 2 was performed from magnetisation data in the temperature range 2 to 15 K, measured in magnetic fields up to 13 T (Fig. 10 and 11). The magnetisation for complexes 1 and 2 reaches values of 12.04 and $18.77 N\beta$ at 13 T, which is below saturation magnetisation (15 and $27 N\beta$, respectively). The observed magnetisation values are close to the theoretically calculated ones, which accounts for antiferromagnetically coupled Cu(II) ions in the metallamacrocycle leading to an $S = 1/2$ state for the Cu_5 cores (11 and $19 N\beta$, respectively). The lower magnetisation value in high field evidences the presence of low-lying excited states with low magnetic moments. Due to the large magnetisation values for complexes 1 and 2 combined with a high metal/ligand mass ratio, these compounds can be considered as possible candidates for magnetic refriger-

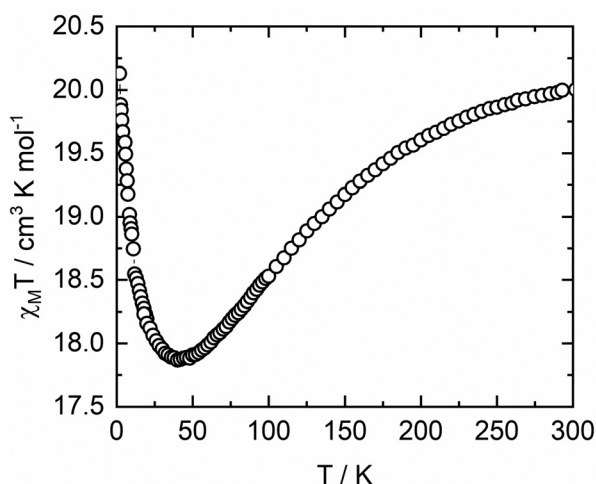


Fig. 8 Thermal dependence of the molar magnetic susceptibility for 2, presented per $\{(\text{GdCu}_5)\text{Cu}\}_2\text{Cu}$ moiety.

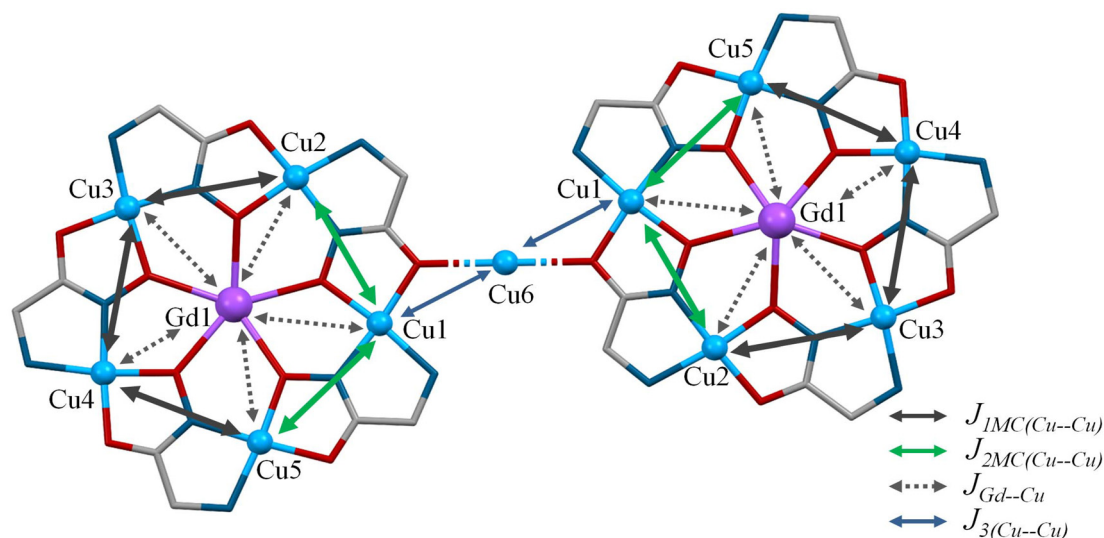


Fig. 9 The scheme for exchange interactions amongst paramagnetic centres in complex 2.



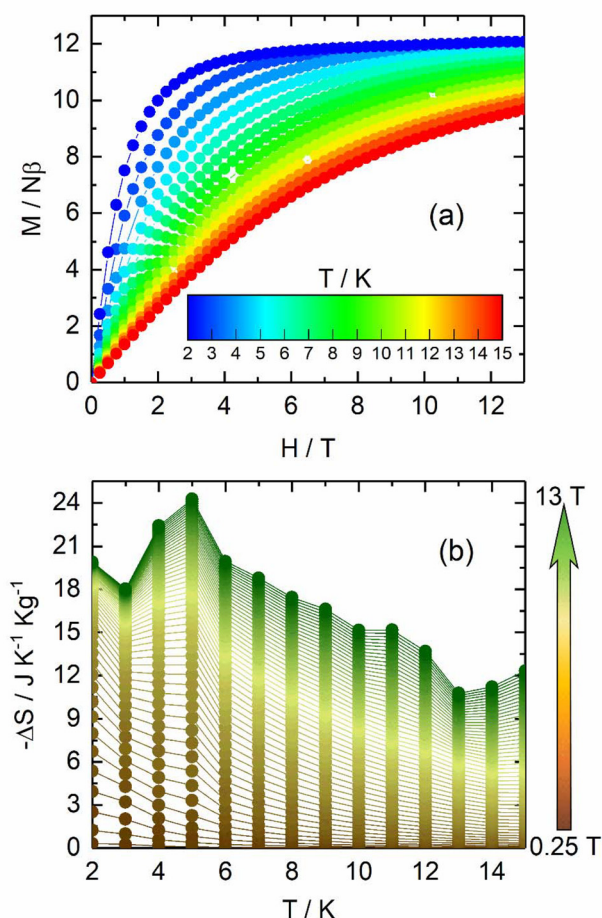


Fig. 10 (a) Field dependence of the magnetisation from 2 to 15 K for **1**. (b) Calculated temperature dependence of magnetic entropy $-\Delta S_m$ obtained from the magnetisation using the Maxwell equations at various fields of 0.25–13 T for **1**.

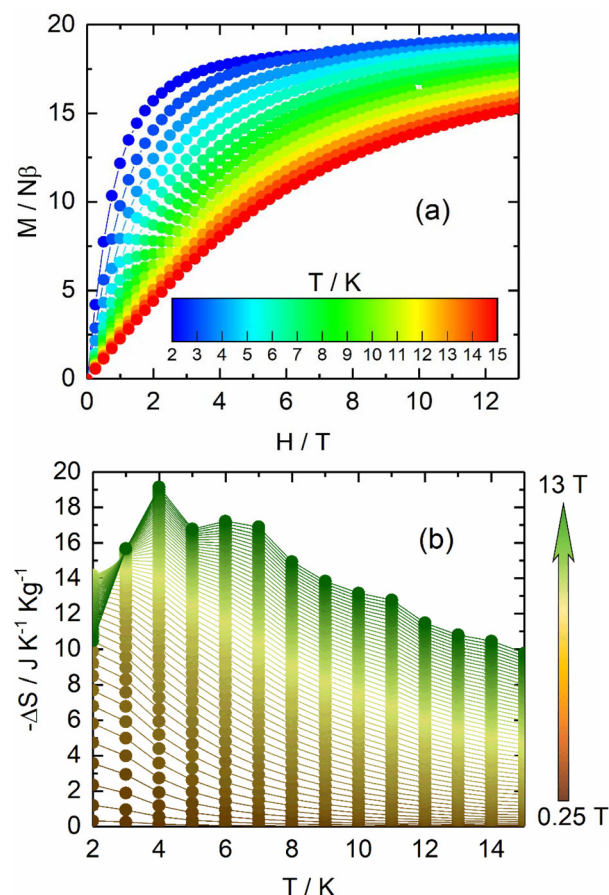


Fig. 11 (a) Field dependence of the magnetisation from 2 to 15 K for **2**. (b) Calculated temperature dependence of magnetic entropy $-\Delta S_m$ obtained from the magnetisation using the Maxwell equations at various fields of 0.25–13 T for **2**.

ation. To evaluate the Magnetocaloric Effect (MCE), the magnetisation data were measured between 2 and 15 K up to a magnetic field of 13 T for both compounds **1** and **2**. The magnetic entropy changes ($-\Delta S_m$) for complexes **1** and **2** were derived from M vs. H data using the Maxwell eqn (2) and (3):^{5,48}

$$\left(\frac{dS}{dB}\right)_T = \left(\frac{dM}{dT}\right)_B \quad (2)$$

$$\Delta S_m(T_0, B) = \int_0^B \left(\frac{dM}{dT}\right)_B dB \quad (3)$$

The dependence of $-\Delta S_m$ on temperature for complexes **1** and **2** is depicted in Fig. 10 and 11, and corresponds to a gradual growth with decreasing temperature and increasing field. The entropy changes for complexes **1** and **2** at 2 K (13 T) are 19.91 J K^{−1} kg^{−1} and 10.48 J K^{−1} kg^{−1} respectively. The maximum $-\Delta S_m$ experimentally observed correspond to 24.26 J K^{−1} kg^{−1} at 5 K (13 T) for **1** and 19.14 J K^{−1} kg^{−1} at 4 K (13 T) for **2**. The observed values for **1** and **2** are lower than the theoretically calculated maximum entropy for non-interacting

paramagnetic ions and were determined from the expression $\Delta S = nR \ln(2S + 1)/M_w$ (where R is the gas constant, n the number of non-interacting spins and M_w is the molar mass) (for complex **1** the theoretical value of $-\Delta S_m$ is $R[\ln(2S_{Gd} + 1) + 5\ln(2S_{Cu} + 1) + \ln(2S_{Cr} + 1)]/M_w = 6.93R/M_w = 37.06$ J K^{−1} kg^{−1}; for **2**: $R[2\ln(2S_{Gd} + 1) + 13\ln(2S_{Cu} + 1)] = 13.17R/M_w = 39.46$ J K^{−1} kg^{−1}). For complexes **1** and **2**, the observed $-\Delta S_m$ values are comparable with the theoretical ones, when five antiferromagnetically coupled Cu(II) ions leading to $S = 1/2$ in a Cu₅ cyclic core [$R[\ln(2S_{Gd} + 1) + \ln(2S_{Cu} + 1) + \ln(2S_{Cr} + 1)] = 4.16R/M_w = 22.21$ J K^{−1} kg^{−1} in **1** and $R[2\ln(2S_{Gd} + 1) + 2\ln(2S_{Cu} + 1) + 3\ln(2S_{Cu} + 1)] = 7.625R/M_w = 21.83$ J K^{−1} kg^{−1} in **2**] are taken into account. The presence of significant antiferromagnetic interaction between the metal centres is generally the origin of the deviation between the maximum calculated and experimental values of $-\Delta S_m$.^{8,49–54} Similar effects on the $-\Delta S_m$ values were observed for Gd(III)–Cu(II) exchange clusters with Cu(II)–Cu(II) exchange interactions as low as -110 cm^{−1}, which led to the stabilization of ground states with lower multiplicities.^{55,56}

Complexes **1** and **2** are the first examples of 15-metallacrown-5 compounds demonstrating a magnetocaloric effect.



The selection of glycinehydroxamic acid, possessing the lowest molecular weight among α -substituted hydroxamic acids needed for the construction of 15-metallacrown-5 cores allows one to obtain polynuclear clusters with high magnetic density, which is favourable for the observation of a significant magnetocaloric effect. The observed values of entropy change for **1** and **2** are comparable with those for 3d–4f polynuclear clusters with similar nuclearity.

Conclusions

Reactions between hexanuclear Gd(III)–Cu(II) 15-metallacrown-5 complexes with anionic oxalate complexes $[\text{Cr}(\text{C}_2\text{O}_4)_3]^{3-}$ and $[\text{Cu}(\text{C}_2\text{O}_4)_2]^{2-}$ led to formation of 1D-polymeric complexes. Studies of magnetic properties in a dc field for the obtained complexes reveal presence of antiferromagnetic exchange interactions between copper(II) ions in the metallamacrocyclic cores and ferromagnetic exchange interactions between Gd(III) and Cu(II) ions. The molecular system **1** allowed us to quantify such magnetic interactions with $J_{\text{Cu–Cu}} = -59.6 \text{ cm}^{-1}$ and $J_{\text{Cu–Gd}} = 0.38 \text{ cm}^{-1}$ as well as the additional magnetic interaction between the Gd(III) and Cr(III) with $J_{\text{Gd–Cr}} = 0.07 \text{ cm}^{-1}$. The isotropic nature of Gd(III) ions and the favorable metal/organic ratio led to the observation of a significant magnetocaloric effect with maximum values of $24.26 \text{ J K}^{-1} \text{ kg}^{-1}$ at 5 K (13 T) for **1** and $19.14 \text{ J K}^{-1} \text{ kg}^{-1}$ at 4 K (13 T) for **2**. The obtained complexes are the first examples of 15-metallacrowns-5 possessing a magnetocaloric effect. The observed values of $-\Delta S_{\text{M}}$ are lower than theoretically estimated for non-coupled paramagnetic centres due to the presence of antiferromagnetic exchange interactions between the paramagnetic centres.

Experimental section

Materials and measurements

Commercially available reagents and solvents (Merck and Aldrich) were used without further purification. The starting complex $[\text{GdCu}_5(\text{GlyHA})_5(\text{CO}_3)(\text{NO}_3)(\text{H}_2\text{O})_5] \cdot 3.5\text{H}_2\text{O}$ was synthesised as described previously.²² C, H, N microanalyses were carried out on a Carlo Erba 1106 instrument. Single-crystal X-ray diffraction was performed at 100 K on a Bruker AXS SMART APEX CCD diffractometer using graphite-monochromated Mo-K α radiation (0.71073 Å). Crystals suitable for X-ray data collection were taken directly from the mother liquor. See the ESI for details on single crystal structure analyses (CCDC 2367413 and 2367414; Table S1†).

The direct current (dc) magnetic susceptibility measurements were performed on solid polycrystalline samples using a Quantum Design MPMS-XL SQUID magnetometer between 2 and 300 K in an applied magnetic field of 0.02 T for temperatures of 2–20 K, 0.2 T for temperatures of 20–80 K and 1 T for temperatures of 80–300 K. Magnetisation data were collected between 2 and 15 K and magnetic fields up to 13 Tesla using a Quantum Design PPMS magnetometers. The sample was

immobilised in a pellet made with Teflon tape. Experimental susceptibility data were corrected for diamagnetic contributions using Pascal's constants.⁵⁷

Synthesis of complex 1. A hot solution of $\text{K}_3[\text{Cr}(\text{C}_2\text{O}_4)_3] \cdot 3.5\text{H}_2\text{O}$ (14.6 mg, 0.03 mmol) in 1 mL H_2O was added to a hot ($\sim 90^\circ\text{C}$) solution of $[\text{GdCu}_5(\text{GlyHA})_5(\text{CO}_3)(\text{NO}_3)(\text{H}_2\text{O})_5] \cdot 3.5\text{H}_2\text{O}$ (25.0 mg, 0.02 mmol) in 2 mL H_2O , followed by addition of 1.5 mL of DMF to the reaction mixture. The solution obtained was stirred for 30 min at $\sim 90^\circ\text{C}$. A small amount of green precipitate was filtered off and the filtrate was left for slow cooling. X-Ray-suitable crystals were obtained after a day. Anal. for $\text{GdCu}_5\text{CrC}_{16}\text{H}_{56}\text{N}_{10}\text{O}_{40}$ exp. (theor.): C: 11.98 (12.35); H: 3.72 (3.63); N: 9.07 (9.01). Yield: 25.8 mg (83%).

Synthesis of complex 2. To a hot ($\sim 90^\circ\text{C}$) solution of $[\text{GdCu}_5(\text{GlyHA})_5(\text{CO}_3)(\text{NO}_3)(\text{H}_2\text{O})_5] \cdot 3.5\text{H}_2\text{O}$ (25.0 mg, 0.02 mmol) in 2 mL distilled H_2O , a hot solution of $\text{K}_2[\text{Cu}(\text{C}_2\text{O}_4)_2] \cdot 2\text{H}_2\text{O}$ (14.4 mg, 0.045 mmol) in 1 mL distilled H_2O was added, followed by addition of 1.5 mL of DMF to the reaction mixture. The resulting solution was stirred for 30 min at $\sim 90^\circ\text{C}$. A small amount of green precipitate was filtered off and the filtrate was left for slow cooling. X-Ray-suitable crystals were obtained after one day. Anal. for $\text{Gd}_2\text{Cu}_{13}\text{C}_{32}\text{H}_{87.60}\text{N}_{20}\text{O}_{67.80}$ exp. (theor.): C: 12.75 (12.97); H: 2.68 (2.92); N: 9.54 (9.45). Yield: 21 mg (71%).

Data availability

Electronic supplementary information (ESI) available: X-ray crystal structure refinement data, analysis of symmetry of coordination environment of metal ions with Shape 2.1 software, IR spectra. Crystallographic data for this paper have been deposited with the CCDC as record 2367413, 2367414 and 2379203.

Conflicts of interest

There are no conflicts to declare.

Acknowledgements

AWA thanks Drexel University for support under the Collaborative Research Agreement between Drexel University College of Arts & Sciences and the Pisarzhevskii Institute of Physical Chemistry.

Funding for this research was partially provided by the National Research Foundation of Ukraine (grant no. 2020.02/0202), The Ukrainian-French R&D joint project for 2021–2022 (no. M/114-2021) and PHC DNIPRO France-Ukraine (no. 46790WL). The X-ray diffractometer (at Youngstown State University) was funded by the National Science Foundation through Grant CHE 0087210, Ohio Board of Regents Grant CAP-491, and by Youngstown State University. AVP thanks Purdue University's Ukrainian Scholars Initiative, Drs. Mike Brzezinski and Jean Chmielewski for providing support and the opportunity to continue research activity.



References

- 1 J.-L. Liu, Y.-C. Chen and M.-L. Tong, Molecular Design for Cryogenic Magnetic Coolants, *Chem. Rec.*, 2016, **16**, 825–834.
- 2 R. Sessoli, Chilling with Magnetic Molecules, *Angew. Chem., Int. Ed.*, 2012, **51**, 43–45.
- 3 P. Konieczny, W. Sas, D. Czernia, A. Pacanowska, M. Fitta and R. Pełka, Magnetic cooling: a molecular perspective, *Dalton Trans.*, 2022, **51**, 12762–12780.
- 4 J.-L. Liu, Y.-C. Chen, F.-S. Guo and M.-L. Tong, Recent advances in the design of magnetic molecules for use as cryogenic magnetic coolants, *Coord. Chem. Rev.*, 2014, **281**, 26–49.
- 5 M. Evangelisti and E. K. Brechin, Recipes for enhanced molecular cooling, *Dalton Trans.*, 2010, **39**, 4672–4676.
- 6 Y.-Z. Zheng, G.-J. Zhou, Z. Zheng and R. E. P. Winpenny, Molecule-based magnetic coolers, *Chem. Soc. Rev.*, 2014, **43**, 1462–1475.
- 7 F.-S. Guo, Y.-C. Chen, L.-L. Mao, W.-Q. Lin, J.-D. Leng, R. Tarasenko, M. Orendáč, J. Prokleška, V. Sechovský and M.-L. Tong, Anion-Templated Assembly and Magnetocaloric Properties of a Nanoscale {Gd₃₈} Cage versus a {Gd₄₈} Barrel, *Chem. – Eur. J.*, 2013, **19**, 14876–14885.
- 8 X.-Y. Zheng, Y.-H. Jiang, G.-L. Zhuang, D.-P. Liu, H.-G. Liao, X.-J. Kong, L.-S. Long and L.-S. Zheng, A Gigantic Molecular Wheel of {Gd₁₄₀}: A New Member of the Molecular Wheel Family, *J. Am. Chem. Soc.*, 2017, **139**(50), 18178–18181.
- 9 S. Zhang and P. Cheng, Coordination-Cluster-Based Molecular Magnetic Refrigerants, *Chem. Rec.*, 2016, **16**, 2077–2126.
- 10 S. K. Langley, N. F. Chilton, B. Moubaraki, T. Hooper, E. K. Brechin, M. Evangelisti and K. S. Murray, Molecular coolers: The case for [Cu^{II}₅Gd^{III}₄], *Chem. Sci.*, 2011, **2**, 1166–1169.
- 11 A. V. Pavlishchuk, S. V. Kolotilov, M. Zeller, L. K. Thompson and A. W. Addison, Formation of Coordination Polymers or Discrete Adducts *via* Reactions of Gadolinium(III)–Copper(II) 15-Metallacrown-5 Complexes with Polycarboxylates: Synthesis, Structures and Magnetic Properties, *Inorg. Chem.*, 2014, **53**, 1320–1330.
- 12 A. V. Pavlishchuk, M. Zeller, L. M. Carrella, E. Rentschler, J. K. Bindra, N. Dalal, J. Kinyon, K. Perera, V. V. Pavlishchuk and A. W. Addison, Structural and Magnetic Properties of a {GdCu₅}₂ Metallacrown Dimer with a Disulfonate Linker, *Eur. J. Inorg. Chem.*, 2024, **27**, e202300544.
- 13 M. Ostrowska, I. O. Fritsky, E. Gumienka-Kontecka and A. V. Pavlishchuk, Metallacrown-based compounds: Applications in catalysis, luminescence, molecular magnetism, and adsorption, *Coord. Chem. Rev.*, 2016, **327–328**, 304–332.
- 14 E. V. Salerno, J. W. Kampf, V. L. Pecoraro and T. Mallah, Magnetic properties of two Gd^{III}Fe^{III}₄ metallacrowns and strategies for optimising the magnetocaloric effect of this topology, *Inorg. Chem. Front.*, 2021, **8**, 2611–2623.
- 15 A. V. Pavlishchuk and V. V. Pavlishchuk, Principles for Creating “Molecular Refrigerators” Derived from Gadolinium(III) Coordination Compounds: A Review, *Theor. Exp. Chem.*, 2020, **56**, 1–25.
- 16 A. V. Pavlishchuk, S. V. Kolotilov, M. Zeller, S. E. Lofland, L. K. Thompson, A. W. Addison and A. D. Hunter, High Nuclearity Assemblies and One-Dimensional (1D) Coordination Polymers Based on Lanthanide–Copper 15-Metallacrown-5 Complexes (Ln^{III} = Pr, Nd, Sm, Eu), *Inorg. Chem.*, 2017, **56**, 13152–13165.
- 17 A. V. Pavlishchuk, S. V. Kolotilov, M. Zeller, S. E. Lofland and A. W. Addison, Magnetic Properties of Ln^{III}–Cu^{II} 15-Metallacrown-5 Dimers with Terephthalate (Ln^{III} = Pr, Nd, Sm, Eu), *Eur. J. Inorg. Chem.*, 2018, 3504–3511.
- 18 J. Jankolovits, C.-S. Lim, G. Mezei, J. W. Kampf and V. L. Pecoraro, Influencing the Size and Anion Selectivity of Dimeric Ln³⁺[15-Metallacrown-5] Compartments through Systematic Variation of the Host Side Chains and Central Metal, *Inorg. Chem.*, 2012, **51**(8), 4527–4538.
- 19 C.-S. Lim, J. Jankolovits, J. Kampf and V. Pecoraro, Chiral Metallacrown Supramolecular Compartments that Template Nanochannels: Self-Assembly and Guest Absorption, *Chem. – Asian J.*, 2010, **5**, 46–49.
- 20 C.-S. Lim, A. C. Van Noord, J. W. Kampf and V. L. Pecoraro, Assessing Guest Selectivity within Metallacrown Host Compartments, *Eur. J. Inorg. Chem.*, 2007, **2007**, 1347–1350.
- 21 B. L. Schneider and V. L. Pecoraro, Host-Guest Chemistry of Metallacrowns, in *Advances in Metallacrown Chemistry*, ed. C. M. Zaleski, Springer Int'l, 2022.
- 22 A. Pavlishchuk, D. Naumova, M. Zeller, S. Calderon Cazorla and A. W. Addison, The crystal structures of {LnCu₅}³⁺ (Ln = Gd, Dy and Ho) 15-metallacrown-5 complexes and a re-evaluation of the isotopic Eu^{III} analogue, *Acta Crystallogr., Sect. E: Crystallogr. Commun.*, 2019, **75**, 1215–1223.
- 23 H. Yang, Y.-X. Meng, H.-Q. Tian, D.-C. Li, S.-Y. Zeng, Y. Song and J.-M. Dou, Investigating the effect of lanthanide radius and diamagnetic linkers on the framework of metallacrown complexes, *Dalton Trans.*, 2020, **49**, 1955–1962.
- 24 A. V. Pavlishchuk, S. V. Kolotilov, M. Zeller, L. K. Thompson, I. O. Fritsky, A. W. Addison and A. D. Hunter, A Triple-Decker Heptadecanuclear (Cu^{II})₁₅(Cr^{III})₂ Complex Assembled from Pentanuclear Metallacrowns, *Eur. J. Inorg. Chem.*, 2010, 4851–4858.
- 25 J. J. Bodwin and V. L. Pecoraro, Preparation of a Chiral, 2-Dimensional Network Containing Metallacrown and Copper Benzoate Building Blocks, *Inorg. Chem.*, 2000, **39**, 3434–3435.
- 26 G. Marinescu, M. Andruh, F. Lloret and M. Julve, Bis (oxalato)chromium(III) complexes: Versatile tectons in designing heterometallic coordination compounds, *Coord. Chem. Rev.*, 2011, **255**(1,2), 161–185.
- 27 E. Pardo, C. Train, G. Gontard, K. Boubekeur, O. Fabelo, H. Liu, B. Dkhil, F. Lloret, K. Nakagawa, H. Tokoro, S.-I. Ohkoshi and M. Verdager, High Proton Conduction in a Chiral Ferromagnetic Metal–Organic Quartz-like Framework, *J. Am. Chem. Soc.*, 2011, **133**(39), 15328–15331.



- 28 S. A. Sahadevan, A. Abhervé, N. Monni, C. S. de Pipaón, J. R. Galán-Mascarós, J. C. Waerenborgh, B. J. C. Vieira, P. Auban-Senzier, S. Pillet, E.-E. Bendeif, P. Alemany, E. Canadell, M. L. Mercuri and N. Avarvari, Conducting Anilate-Based Mixed-Valence Fe(II)Fe(III) Coordination Polymer: Small-Polaron Hopping Model for Oxalate-Type Fe(II)Fe(III) 2D Networks, *J. Am. Chem. Soc.*, 2018, **140**(39), 12611–12621.
- 29 S.-J. Liu, X.-R. Xie, T.-F. Zheng, J. Bao, J.-S. Liao, J.-L. Chen and H.-R. Wen, Three-dimensional two-fold interpenetrated Cr^{III}–Gd^{III} heterometallic framework as an attractive cryogenic magnetorefrigerant, *CrystEngComm*, 2015, **17**, 7270–7275.
- 30 A. V. Pavlishchuk, S. V. Kolotilov, I. O. Fritsky, M. Zeller, A. W. Addison and A. D. Hunter, Structural trends in a series of isostructural lanthanide-copper metallacrown sulfates (Ln^{III} = Pr, Nd, Sm, Eu, Gd, Dy and Ho): hexaaqua-pentakis[μ₃-glycinehydroxamato(2-)]sulfatopentacopper(II) lanthanide(III) hepta-aqua-pentakis[μ₃-glycinehydroxamato(2-)]sulfatopentacopper(II)lanthanide(III) sulfate hexahydrate, *Acta Crystallogr., Sect. C: Cryst. Struct. Commun.*, 2011, **67**, m255–m265.
- 31 A. D. Cutland, J. A. Halfen, J. W. Kampf and V. L. Pecoraro, Chiral 15-Metallacrown-5 Complexes Differentially Bind Carboxylate Anions, *J. Am. Chem. Soc.*, 2001, **123**, 6211–6212.
- 32 A. V. Pavlishchuk, I. V. Vasylenko, M. Zeller and A. W. Addison, Crystal structure of a Tb^{III}–Cu^{II} glycinehydroxamate 15-metallacrown-5 sulfate complex, *Acta Crystallogr., Sect. E: Crystallogr. Commun.*, 2021, **77**, 1197–1202.
- 33 D. Casanova, M. Llunell, P. Alemany and S. Alvarez, The Rich Stereochemistry of Eight-Vertex Polyhedra: A Continuous Shape Measures Study, *Chem. – Eur. J.*, 2005, **11**, 1479–1494.
- 34 A. L. Spek, *PLATON – A Multipurpose Crystallographic Tool*, Utrecht University, The Netherlands, 2006.
- 35 R. Lescouëzec, G. Marinescu, J. Vaissermann, F. Lloret, J. Faus, M. Andruh and M. Julve, [Cr(AA)(C₂O₄)₂][–] and [Cu(bpca)]⁺ as building blocks in designing new oxalato-bridged Cr^{III}Cu^{II} compounds [AA = 2,2'-bipyridine and 1,10-phenanthroline; bpca = bis(2-pyridylcarbonyl)amide anion], *Inorg. Chim. Acta*, 2003, **350**, 131–142.
- 36 G. Marinescu, M. Andruh, F. Lloret and M. Julve, Bis(oxalato)chromium(III) complexes: Versatile tectons in designing heterometallic coordination compounds, *Coord. Chem. Rev.*, 2011, **255**, 161–185.
- 37 L. Kanižaj, K. Molčanov, F. Torić, D. Pajić, I. Lončarić, A. Šantić and M. Jurić, Ladder-like [CrCu] coordination polymers containing unique bridging modes of [Cr(C₂O₄)₃]^{3–} and Cr₂O₇^{2–}, *Dalton Trans.*, 2019, **48**, 7891–7898.
- 38 N. F. Chilton, R. P. Anderson, L. D. Turner, A. Soncini and K. S. Murray, PHI: A powerful new program for the analysis of anisotropic monomeric and exchange-coupled polynuclear d- and f-block complexes, *J. Comput. Chem.*, 2013, **34**, 1164–1175.
- 39 The measure of the deviation of the fit is $R^2 = \sum[(\chi_M T)_{\text{obs.}} - (\chi_M T)_{\text{calc.}}]^2 / (\sum(\chi_M T)_{\text{obs.}}^2)$.
- 40 J. Wang, Q.-W. Li, S.-G. Wu, Y.-C. Chen, R.-C. Wan, G.-Z. Huang, Y. Liu, J.-L. Liu, D. Reta, M. J. Giansiracusa, Z.-X. Wang, N. F. Chilton and M.-L. Tong, Opening Magnetic Hysteresis by Axial Ferromagnetic Coupling: From Mono-Decker to Double-Decker Metallocrown, *Angew. Chem., Int. Ed.*, 2021, **60**, 5299–5306.
- 41 J. Wang, Z.-Y. Ruan, Q.-W. Li, Y.-C. Chen, G.-Z. Huang, J.-L. Liu, D. Reta, N. F. Chilton, Z.-X. Wang and M.-L. Tong, Slow magnetic relaxation in a {EuCu₅} metallocrown, *Dalton Trans.*, 2019, **48**, 1686–1692.
- 42 C. Benelli and D. Gatteschi, Magnetism of Lanthanides in Molecular Materials with Transition-Metal Ions and Organic Radicals, *Chem. Rev.*, 2002, **102**, 2369–2387.
- 43 (a) G. Rajaraman, F. Totti, A. Bencini, A. Caneschi, R. Sessoli and D. Gatteschi, Density functional studies on the exchange interaction of a dinuclear Gd(III)–Cu(II) complex: method assessment, magnetic coupling mechanism and magneto-structural correlations, *Dalton Trans.*, 2009, 3153–3161; (b) A. Panja, S. Paul, E. Moreno-Pineda, R. Herchel, N. C. Jana, P. Brandão, G. Novitchi and W. Wernsdorfer, Insight into ferromagnetic interactions in Cu^{II}–Ln^{III} dimers with a compartmental ligand, *Dalton Trans.*, 2024, **53**, 2501–2511.
- 44 (a) M. J. H. Ojea, C. Wilson, J. Cirera, H. Oshio, E. Ruiz and M. Murrie, Elucidating the exchange interactions in a {Gd^{III}Cu^{II}₄} propeller, *Dalton Trans.*, 2023, **52**, 3203–3209; (b) V. Béreau, S. Dhers, J.-P. Costes, C. Duhayon and J.-P. Sutter, Syntheses, Structures, and Magnetic Properties of Symmetric and Dissymmetric Ester-Functionalized 3d-4f Schiff Base Complexes, *Eur. J. Inorg. Chem.*, 2018, **2018**, 66–73; (c) J. Zhang, C. Li, J. Wang, M. Zhu and L. Li, Slow Magnetic Relaxation Behavior in Rare Ln–Cu–Ln Linear Trinuclear Complexes, *Eur. J. Inorg. Chem.*, 2016, **2016**, 1383–1388; (d) D. Visinescu, A. Madalan, M. Andruh, C. Duhayon, J.-P. Sutter, L. Ungur, W. Van den Heuvel and L. Chibotaru, First Heterotrimetallic {3d-4d-4f} Single Chain Magnet, Constructed from Anisotropic High-Spin Heterometallic Nodes and Paramagnetic Spacers, *Chem. – Eur. J.*, 2009, **15**, 11808–11814; (e) O. Iasco, G. Novitchi, E. Jeanneau and D. Luneau, Lanthanide Triangles Sandwiched by Tetranuclear Copper Complexes Afford a Family of Hendecanuclear Heterometallic Complexes [Ln^{III}₃Cu^{II}₄] (Ln = La–Lu): Synthesis and Magnetostructural Studies, *Inorg. Chem.*, 2013, **52**, 8723–8731.
- 45 (a) T. N. Hooper, R. Inglis, G. Lorusso, J. Ujma, P. E. Barran, D. Uhrin, J. Schnack, S. Piligkos, M. Evangelisti and E. K. Brechin, Structurally Flexible and Solution Stable [Ln₄TM₈(OH)₈(L)₈(O₂CR)₈(MeOH)_y](ClO₄)₄: A Playground for Magnetic Refrigeration, *Inorg. Chem.*, 2016, **55**, 10535–10546; (b) P. Richardson, D. I. Alexandropoulos, L. Cunha-Silva, G. Lorusso, M. Evangelisti, J. Tang and T. C. Stamatatos, 'All three-in-one': ferromagnetic interactions, single-molecule magnetism and magnetocaloric properties in a new family of



- [Cu₄Ln] (Ln^{III} = Gd, Tb, Dy) clusters, *Inorg. Chem. Front.*, 2015, **2**, 945–948; (c) T. N. Hooper, R. Inglis, M. A. Palacios, G. S. Nichol, M. B. Pitak, S. J. Coles, G. Lorusso, M. Evangelisti and E. K. Brechin, CO₂ as a reaction ingredient for the construction of metal cages: a carbonate-panelled [Gd₆Cu₃] tridimensional icosahedrons, *Chem. Commun.*, 2014, **50**, 3498–3500.
- 46 (a) P. Shukla, S. Das, P. Bag and A. Dey, Magnetic materials based on heterometallic Cr^{III}–Ln^{III} complexes, *Inorg. Chem. Front.*, 2023, **10**, 4322–4357; (b) K. S. Pedersen, G. Lorusso, J. J. Morales, T. Weyhermüller, S. Piligkos, S. K. Singh, D. Larsen, M. Schau-Magnussen, G. Rajaraman, M. Evangelisti and J. Bendix, Fluoride-Bridged {Gd^{III}₃M^{III}₂} (M=Cr, Fe, Ga) Molecular Magnetic Refrigerants, *Angew. Chem., Int. Ed.*, 2014, **53**, 2394–2397; (c) O. Blacque, A. Amjad, A. Caneschi, L. Sorace and P.-E. Car, Synthesis, structure, magnetic and magnetocaloric properties of a series of {Cr^{III}₄Ln^{III}} complexes, *New J. Chem.*, 2016, **40**, 3571–3577; (d) D. Chauhan, K. R. Vignesh, A. Swain, S. K. Langley, K. S. Murray, M. Shanmugam and G. Rajaraman, Exploiting Strong {Cr^{III}–Dy^{III}} Ferromagnetic Exchange Coupling to Quench Quantum Tunneling of Magnetization in a Novel {Cr^{III}₂Dy^{III}₃} Single-Molecule Magnet, *Cryst. Growth Des.*, 2023, **23**, 197–206.
- 47 (a) J. H. Mucchia Ortiz, D. Cabrosi, L. M. Carrella, E. Rentschler and P. Alborés, SMM Behaviour of the Butterfly {Cr^{III}₂Dy^{III}₂} Pivalate Complex and Magneto-structurally Correlated Relaxation Thermal Barrier, *Chem. – Eur. J.*, 2022, **28**, e202201450; (b) T. Birk, K. S. Pedersen, C. A. Thuesen, T. Weyhermüller, M. Schau-Magnussen, S. Piligkos, H. Weihe, S. Mossin, M. Evangelisti and J. Bendix, Fluoride Bridges as Structure-Directing Motifs in 3d-4f Cluster Chemistry, *Inorg. Chem.*, 2012, **51**, 5435–5443; (c) J.-J. Yin, C. Chen, G.-L. Zhuang, J. Zheng, X.-Y. Zheng and X.-J. Kong, Anion-Dependent Assembly of 3d-4f Heterometallic Clusters Ln₅Cr₂ and Ln₈Cr₄, *Inorg. Chem.*, 2020, **59**, 1959–1966; (d) C. Chen, Y. Liu, P. Li, H. Zhou and X. Shen, Construction of Ni^{II}Ln^{III}M^{III} (Ln = Gd^{III}, Tb^{III}; M = Fe^{III}, Cr^{III}) clusters showing slow magnetic relaxations, *Dalton Trans.*, 2015, **44**, 20193–20199.
- 48 H. B. Callen, *Thermodynamics and an Introduction to Thermostatistics*, 1998, pp. 164–167.
- 49 H.-M. Chen, W.-M. Wang, X.-Q. Li, X.-Y. Chu, Y.-Y. Nie, Z. Liu, S.-X. Huang, H.-Y. Shen, J.-Z. Cui and H.-L. Gao, Luminescence and magnetocaloric effect of Ln₄ clusters (Ln = Eu, Gd, Tb, Er) bridged by CO₃²⁻ deriving from the spontaneous fixation of carbon dioxide in the atmosphere, *Inorg. Chem. Front.*, 2018, **5**, 394–402.
- 50 H.-L. Gao, N.-N. Wang, W.-M. Wang, H.-Y. Shen, X.-P. Zhou, Y.-X. Chang, R.-X. Zhang and J.-Z. Cui, Finetuning the magnetocaloric effect and SMMs behaviors of coplanar RE₄ complexes by β -diketonate coligands, *Inorg. Chem. Front.*, 2017, **4**, 860–870.
- 51 J. Wu, X.-L. Li, L. Zhao, M. Guo and J. Tang, Enhancement of Magnetocaloric Effect through Fixation of Carbon Dioxide: Molecular Assembly from Ln₄ to Ln₄ Cluster Pairs, *Inorg. Chem.*, 2017, **56**, 4104–4111.
- 52 X.-M. Luo, Z.-B. Hu, Q.-F. Lin, W. Cheng, J.-P. Cao, C.-H. Cui, H. Mei, Y. Song and Y. Xu, Exploring the Performance Improvement of Magnetocaloric Effect Based Gd-Exclusive Cluster Gd₆₀, *J. Am. Chem. Soc.*, 2018, **140**, 11219–11222.
- 53 J.-B. Peng, X.-J. Kong, Q.-C. Zhang, M. Orendáč, J. Prokleška, Y.-P. Ren, L.-S. Long, Z. Zheng and L.-S. Zheng, Beauty, Symmetry, and Magnetocaloric Effect – Four-Shell Keplers with 104 Lanthanide Atoms, *J. Am. Chem. Soc.*, 2014, **136**, 17938–17941.
- 54 P. Kumar, J. Flores Gonzalez, P. Prakash Sahu, N. Ahmed, J. Acharya, V. Kumar, O. Cadot, F. Pointillart, S. Kumar Singh and V. Chandrasekhar, Magnetocaloric effect and slow magnetic relaxation in peroxide-assisted tetranuclear lanthanide assemblies, *Inorg. Chem. Front.*, 2022, **9**, 5072–5092.
- 55 (a) T. Rajeshkumar, H. V. Annadata, M. Evangelisti, S. K. Langley, N. F. Chilton, K. S. Murray and G. Rajaraman, Theoretical Studies on Polynuclear {Cu^{II}₅Gd^{III}_n} Clusters (n = 4, 2): Towards Understanding Their Large Magnetocaloric Effect, *Inorg. Chem.*, 2015, **54**, 1661–1670; (b) A. Dey, S. Das, M. A. Palacios, E. Colacio and V. Chandrasekhar, Single-Molecule Magnet and Magnetothermal Properties of Two-Dimensional Polymers Containing Heterometallic [Cu₅Ln₂] (Ln = Gd^{III} and Dy^{III}) Motifs, *Eur. J. Inorg. Chem.*, 2018, **2018**, 1645–1654; (c) S. Xue, Y.-N. Guo, L. Zhao, H. Zhang and J. Tang, Molecular Magnetic Investigation of a Family of Octanuclear [Cu₆Ln₂] Nanoclusters, *Inorg. Chem.*, 2014, **53**, 8165–8171.
- 56 J.-D. Leng, J.-L. Liu and M.-L. Tong, Unique nanoscale {Cu^{II}₃₆Ln^{III}₂₄} (Ln = Dy and Gd) metallo-rings, *Chem. Commun.*, 2012, **48**, 5286–5288.
- 57 O. Kahn, *Molecular Magnetism*, VCH Publishers Inc., Weinheim, 1993.

